Fission time scale and viscosity for compound nucleus ^{220}Th formed in reaction ^{40}Ar+^{180}Hf at E_{lab}= 180, 190, 216, and 249 MeV

V. A. Rubchenya,[1,2] A. V. Kuznetsov,[1,2] W. H. Trzaska,[1] D. N. Vakhtin,[1,2] A. A. Alexandrov,[3] I. D. Alkhazov,[2] J. Äystö,[1] S. V. Khlebnikov,[2] V. G. Lyapin,[2] O. I. Osetrov,[2] Yu. E. Penionzhkevich,[3] Yu. V. Pyatkov,[3] and G. P. Tiourin[2]

[1]*Department of Physics, University of Jyväskylä, FIN-40351, Jyväskylä, Finland*
[2]*V.G. Khlopin Radium Institute, 194021, St. Petersburg, Russia*
[3]*Flerov Laboratory of Nuclear Reactions, 149980, Dubna, Russia*
(Received 5 December 1997)

Double differential spectra of neutrons emitted from the reaction ^{40}Ar+^{180}Hf at E_{lab}=180, 190, 216, and 249 MeV were measured in coincidence with fission fragments using a multidetector array. Averaged prescission and postscission neutron multiplicites were extracted from the spectra together with temperature parameters. These values were analyzed in the framework of a modified version of the statistical model with inclusion of dynamical hindrance of fission, which depends on nuclear dissipation. From comparison of the experimental and calculated neutron multiplicities and temperatures it was deduced that nuclear viscosity is strong at excitation energies higher than $\sim$40 MeV and decreases with the decrease of excitation energy during evaporation cascade. The extracted fission time scale changes from 40×10^{-20} s to 17×10^{-20} s in the investigated projectile energy interval. [S0556-2813(98)03909-0]

PACS number(s): 25.70.Jj, 25.85.Ge, 24.10.Pa, 24.75.+i

I. INTRODUCTION

Studies of heavy-ion-induced fusion-fission reactions became the main method to investigate large scale collective nuclear motion. The main goal of these studies is the extraction of statistical and dynamical parameters of nuclear matter at different stages of the fusion-fission process. Neutrons, protons, α particles, and high-energy γ rays are used as probes of nuclear temperature and time scale in heavy-ion-induced fusion-fission reactions [1,2]. As compared to standard statistical model predictions, there is a clear excess of prescission multiplicities of light particles and γ quanta [1,2]. This excess indicates dynamic hindrance of fission process possibly caused by (i) retardation in the formation of fission degrees of freedom, (ii) dissipation effects during collective motion towards the barrier and scission point, and (iii) light particle and γ quanta emission at the descent stage between the saddle and scission points.

The main bulk of information about fission time scale of heated rotating nuclei formed in heavy-ion-induced fusion-fission reactions has been obtained with neutron measurements [1]. From comparison of these data with a theoretical model calculation one can derive the prescission time scale and friction coefficient. One of the important problems in the fission dynamics is the dependence of friction parameter on the shape and temperature. However, conclusions about nature and strength of nuclear friction are still ambiguous [3] and additional work in this direction is needed.

Only a few neutron measurements in ^{40}Ar-induced fusion-fission reactions on ^{141}Pr, ^{169}Tm, ^{165}Ho, ^{181}Ta, ^{197}Au, ^{208}Pb, and $^{\text{nat}}$U targets at E_{lab}=249 MeV [4] and E_{lab}=216 MeV on ^{180}Hf [5] were carried out. Up to present there has been no measurements for different ^{40}Ar-beam energies on the same target although an excitation function of fusion-fission process characteristics is more informative. In order to understand better the dynamics of a fusion-fission process, we undertook the investigation of the reaction ^{40}Ar+^{180}Hf at beam energies ranging from just above the

fission barrier up to 249 MeV. The neutron measurements for this reaction were made for the first time and they are of special interest because the compound nucleus ^{220}Th lies near the maximum of prescission neutron multiplicity dependence on compound nucleus mass M_n^{pre} (A_{CN}) observed by Hinde *et al.* [4]. Our first results of the measurements at E_{lab}(^{40}Ar)=216 MeV [5] were remeasured with more advanced technique. Interpretation of the data is based on model calculations using a new code SCRONMCD (statistical calculations for rotating nuclei by Monte Carlo method with dynamics) [6] that allows us to extract energy dependence of fission time scale from the measured prescission and postscission neutron multiplicities and evaporation residue (ER) formation cross sections.

II. EXPERIMENT

The measurements were carried out using the HENDES (High Efficiency Neutron Detection System) facility [7] at the Department of Physics, University of Jyväskylä. The scheme of the experimental setup is shown in Fig. 1. A 45 μg/cm^2 layer of ^{180}Hf evaporated on 70 μg/cm^2 thick Al$_2$O$_3$ backing was bombarded with 180, 190, 216, and 249 MeV beams of ^{40}Ar. A typical beam spot diameter on the target was 5 mm, the average beam intensity was about 5 particle nA. To measure double-differential neutron spectra (recording both energy and angle) in coincidence with fission fragments, two large, position sensitive avalanche counters (PSACs) [8], five position sensitive neutron detectors (PSNDs) [9], and one microchannel plate (MCP) start detector were used.

The time-of-flight (TOF) method was used for detection of fission fragments and neutrons. In order to separate fission from other possible reaction channels good knowledge of fragment velocity vectors $\vec{v}_f$ was required. Also, sufficient statistics was needed to carry out reliable unfolding of the spectra into prescission and postscission components. For both PSACs, the distance between the cathode's center and the target was 230 mm. The in-plane angles between the
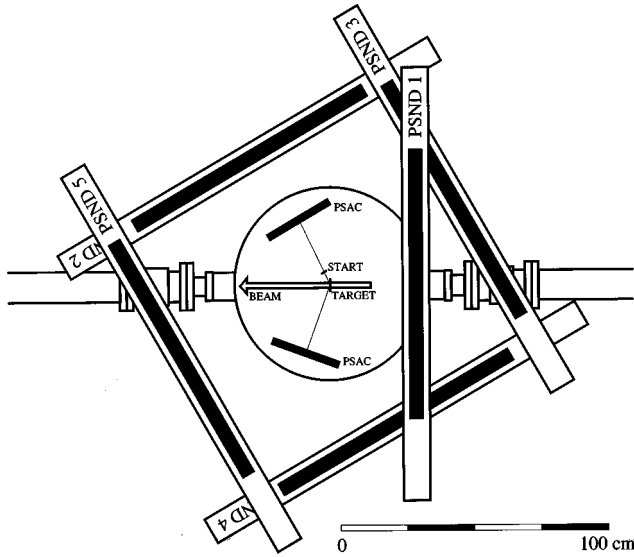
FIG. 1. HENDES array: experimental lay-out during the ^{40}Ar$+^{180}$Hf experiment.

beam direction and centers of the first and second PSACs were $-60°$ and $+70°$, respectively. The angular acceptance of both detectors was $56°$ in-plane and $\pm 28°$ out-of-plane. These angles were chosen to allow the detection of only some elastically scattered particles as a reference point for the subsequent data analysis. Both the PSACs and the MCP detector were placed inside a spherical, stainless steel reaction chamber with a diameter of 80 cm and wall thickness of 2 mm.

Neutron energy determination was also based on the TOF technique as described in our previous work [5]. The energy-dependent position resolution of our neutron detectors changes from 20 cm for 1 MeV neutrons to 10 cm for 4 MeV neutron energies and above. This makes the set of 5 PSNDs equivalent to at least 25 individual detectors. We have also estimated the influence of the reaction chamber and other surrounding materials on the registration of neutron spectra. About 10^5 events of triple coincidences between two complementary heavy fission fragments and a neutron at both 216 and 249 MeV and about 2×10^4 events at 180 and 190 MeV were collected. The total number of coincidences between two fission fragments was considerably higher and provided normalization for the neutron spectra.

III. DATA ANALYSIS AND EXPERIMENTAL RESULTS

A. Fission fragments

The aim of the analysis of fission fragment data was to determine primary fragment masses m_1 and m_2 and velocity vectors $\vec{v}_1$ and $\vec{v}_2$. It was done with a successive approximation method. In the zero approximation, fragment velocity vector $\vec{v}_f^0$ was determined from the time of flight and from the registration coordinates. The main source of error at this stage comes from unaccounted energy loss in the START detector converter foil and in the target ($\Delta E \approx 5$ MeV for symmetrical mass split in both cases).

The first approximation for fragment masses $m_{1,2}^0$ was calculated using momentum conservation perpendicular to the

beam axis $m_1 v_1^\perp = m_2 v_2^\perp$ and assuming that the two fragment masses add up to the mass of the compound system prior to fission ($m_1 + m_2 = M_{\text{projectile}} + M_{\text{target}} - \langle M^{\text{pre}} \rangle$), where $\langle M^{\text{pre}} \rangle$ is the mean total mass of particles evaporated from the compound nucleus before scission. Since, according to our model predictions, neutrons dominate in prescission emission and $\langle M^{\text{pre}} \rangle$ was assumed to be equal to neutron prescission multiplicity $\langle M_n^{\text{pre}} \rangle$. The value of $\langle M_n^{\text{pre}} \rangle$ was first taken from theoretical calculations and, at a later stage, substituted with the experimental value. The influence of uncertainty in $\langle M^{\text{pre}} \rangle$ determination turned out to be much smaller than the overall errors determined mostly by the time resolution of PSACs.

From $\vec{v}_{1,2}^0$ and $m_{1,2}^0$ fragment energies $E_{1,2}^0$ were determined using nonrelativistic formulas. Known fragment mass and energy allowed us to calculate consequently the energy losses in the START detector and the target. From the corrected values of $E_{1,2}^1 = E_{1,2}^0 + \Delta E^{\text{START}} + \Delta E^{\text{target}}$ and old values of fragment masses $m_{1,2}^0$, new values of the fragment velocities ''in the target'' were calculated; the above procedure was repeated until it converged. Usually, two iterations were sufficient. Using the extracted values of $\vec{v}_{1,2}$ and $m_{1,2}$, experimental laboratory velocity of the compound nuclear system $\vec{V}_{\text{CN}}$, fragment velocities in the center of mass, and a total kinetic energy (TKE) distribution of fission fragments were calculated. Separation fission events from full fusion compound nucleus had been made by requiring folding angle between two fission fragments to be distributed around the value corresponding to complete fusion. The fact that experimentally measured velocity of the compound system is centered around the value expected for full linear momentum transfer supports the assumption that contribution of reaction mechanisms with incomplete fusion is small. The mean value of total kinetic energy of the fission fragments $\langle \text{TKE} \rangle = (166 \pm 4)$ MeV for all energies was found to be in agreement with Viola systematics [10]. A full width at half maximum (FWHM) of the primary fission fragment distribution was found to be 42.3 u, which is consistent with the FWHM$=43.3$ u obtained earlier by us at $E_{\text{lab}} = 216$ MeV (see Ref. [5]).

B. Neutron spectra

Each neutron event consisted of six parameters; three from each of the two photomultipliers at the opposite ends of PSND: time, total, and fast components of the charge pulse. Standard pulse shape analysis was used to separate neutrons from γ quanta.

In the analysis of neutron events, each PSND was treated as five separate detectors. Energy- and position-dependent efficiency was calculated with SITHA (simulation transport of hadron) code [11] which uses a multigroup approach based on the neutron cross section library GR175-V1, and the response functions of the NE-213 scintillator [12]. Prior to the experiment, the influence of 2 mm stainless steel walls of the reaction chamber on neutron spectra was measured, and energy- and position-dependent corrections were extracted. ^{252}Cf test was always used as a reference. From the measured neutron spectra and from the well-known parameters of ^{252}Cf neutron emission, experimental PSND efficiency
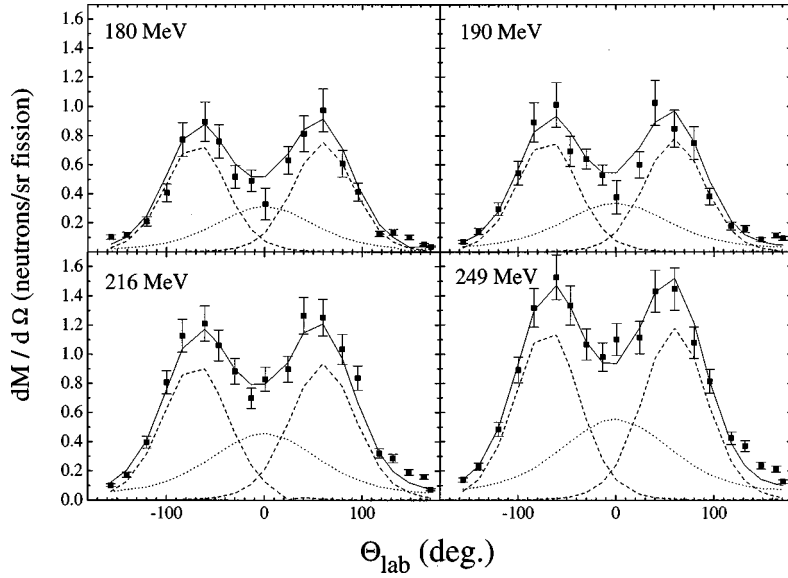
FIG. 2. Measured angular dependence of neutron multiplicities at $E_{\text{lab}} = 180$, 190, 216, and 249 MeV. The contributions of different sources as obtained from the multiple-source fit are shown by lines: full lines: total, dashed lines: postscission, dotted lines: prescission.

was extracted. The result was in agreement with SITHA calculations. At low neutron energies (around 1 MeV) the main source of the 13% error in energy determination is due to the uncertainty of the flight path. At higher energies (about 10 MeV) the errors are mostly due to finite time resolution (1.4 ns for all detectors) and amount to about 15%.

To extract prescission and postscission neutron multiplicities and temperature parameters, a multiple-source procedure was used. Neutrons were assumed to be emitted isotropically in corresponding rest frames of three moving sources: compound nucleus and two fully accelerated fission fragments. Contribution of preequilibrium emission was estimated to be small ($M_n^{\text{preeq}} < 0.3$) [4]; furthermore, due to the relatively high energy of these neutrons their contribution in the neutron energy range used for least-square fitting procedure (2–7 MeV) can be neglected. The following fitting formula was used:

$$\frac{d^2 M_n}{dE_n d\Omega_n} = \frac{M_n^{\text{pre}} \sqrt{E_n \epsilon_n}}{4\pi (T^{\text{pre}})^2} \exp\left(-\frac{\epsilon_n}{T^{\text{pre}}}\right)$$
$$+ \sum_{i=1}^{2} \frac{M_{n,i}^{\text{post}} \sqrt{E_n}}{2(\pi T^{\text{post}})^{3/2}} \exp\left(-\frac{\epsilon_n}{T^{\text{post}}}\right), \quad (3.1)$$

where $\epsilon_n = E_n - 2\sqrt{E_n E_{C(F)}/A_{C(F)}} \cos(\Phi_{C(F)}) + E_{C(F)}/A_{C(F)}$, E_n is the neutron energy in the lab system, T^{pre} is the average temperature of the compound nucleus, T^{post} is the average temperature of fission fragments, E_C is the average kinetic energy of the compound nucleus, E_F is the average kinetic energy of fission fragments, A_C is the mass of the compound nucleus, A_F is the average mass of a fission fragment, and $\Phi_{C(F)}$ is the angle between neutron direction and compound nucleus (fragment) velocity direction.

Such a parametrization was chosen to provide the best fit to measured neutron energy spectra. However, different spectral shapes for prescission and postscission components have little influence on data in 2–7 MeV energy range which was used for spectrum deconvolution.

A nearly perfect 360° coverage in the horizontal plane allowed us to build full neutron angular distribution thus assuring good data for the fitting procedure. In the fit only

neutrons with energies greater than 2 MeV were taken into account in order to reduce the influence of data points close to the registration threshold. Neutron multiplicities (integrated for all energies) as a function of laboratory angle are shown in Fig. 2. Experimentally obtained values of prescission, postscission, and total neutron multiplicities and temperature parameters are summarized in Table I. The values of M_n^{pre} and M_n^{post} for $E_{\text{lab}} = 216$ MeV are different from those reported by us in Ref. [5]. The reason for that seems to be twofold: (a) much higher statistics collected in present work due to high efficiency fission fragment detectors and addition of two more PSNDs; (b) a much more reliable deconvolution procedure used in present work, which relies on angular distribution of neutrons (see Fig. 2) and is much less sensitive to spectral shape close to registration threshold.

IV. THEORETICAL MODEL ANALYSIS

To make estimations of fission time scale and friction strength from obtained experimental data the new method and calculation code SCRONMCD [5,6] were used. The fusion-fission process is supposed to go through four main stages: formation of compound nucleus in the heavy-ion collision, deexcitation stage near equilibrium deformation of compound nucleus and formation of fission degrees of freedom, deexcitation process at the descent from the saddle to scission point, and relaxation of fission fragments after scission. In heavy-ion fusion reactions at low bombarding energy (E

TABLE I. Prescission and postscission neutron multiplicities M_n and temperature parameters T obtained from the multiple-source fit. Errors were deduced from χ^2 behavior (increase by 3% from the minimum value).

E_{lab} (MeV)	M_n^{pre}	M_n^{post}	M_n^{tot}	T^{pre} (MeV)	T^{post} (MeV)
180	1.7 ± 0.3	4.2 ± 0.3	5.9 ± 0.4	1.0 ± 0.2	0.9 ± 0.2
190	1.8 ± 0.3	4.3 ± 0.3	6.2 ± 0.4	1.3 ± 0.2	1.0 ± 0.1
216	2.3 ± 0.4	5.9 ± 0.4	8.2 ± 0.6	1.4 ± 0.2	1.1 ± 0.2
249	3.6 ± 0.4	6.5 ± 0.4	10.1 ± 0.6	1.6 ± 0.2	1.2 ± 0.2

≤ 10 MeV/nucleon) the formation and deexcitation stages are totally decoupled and these two phases are separated by several orders of magnitude in time. Hence the fission time (prescission time) is decomposed into two parts

$$T_f = T_{eq \to sd} + T_{sd \to sc}, \qquad (4.1)$$

where $T_{eq \to sd}$ is time needed for transition from equilibrium compound state to saddle point and $T_{sd \to sc}$ is time of the descent from saddle to scission point. The method for calculating averaged fission time and measured fission characteristics was presented in Ref. [6] and is briefly described below.

The fusion cross section is calculated by Swiatecki's extra-push model [13] using the proximity approximation [14] for nuclear part of the nucleus-nucleus interaction. The partial fusion cross section $\sigma_{fus}(I)$ parametrized by two values (critical fusion angular momentum I_{cr} and diffuseness parameter of angular momentunm distribution d_I) is determined by adjusting calculated fusion cross section. A liquid drop model fission barrier is calculated for symmetrical fission using an parametrization in lemniscate coordinates [15] taking into account the temperature dependence of potential energy in the Thomas-Fermi model approximation [16]. In addition, a scale factor C_b for a liquid drop model fission barrier is used as an adjusting parameter. A rigid-body momentum of inertia used for evaluation of rotation energy was calculated taking into account the diffuseness of nuclear matter distribution.

The light particles and γ-ray emission are assumed to start with their full statistical decay widths at time $t = 0$ when the compound nucleus is formed at near equilibrium deformation at given angular momentum I. The stationary fission probability flow over the fission barrier approaches the asymptotic value after some delay time. The time-dependent fission width is determined by the expression [17,18]

$$\Gamma_f(t) = \Gamma_f^{BW}[1 - \exp(-t/\tau_d)][(1+\gamma^2)^{1/2} - \gamma]. \quad (4.2)$$

Here τ_d is a time delay parameter, Γ_f^{BW} is a statistical Bohr-Wheeler fission width, and γ is a nuclear friction coefficient $\gamma = \beta/2\omega_b$; β denotes the reduced dissipation coefficient and ω_b describes the potential curvature at the fission saddle point. For all decay channels level densities were calculated using the parametrization proposed in Ref. [19]. To calculate Γ_f^{BW} the scale factor for level density parameter is introduced $a_f = C_a a_{eq}$ and zero values of shell corrections were used. The change of angular momentum after emission of particles or γ quanta with energy ϵ is taken into account in average, assuming that $\Delta I = 1$ for the giant-dipole-resonance (GDR) γ ray and for particles $\Delta I \sim \sqrt{\epsilon}$. The parameters of the GDR strength function have been chosen supposing a collective prolate shape for compound nucleus and a spherical shape for fission fragments.

After passing the saddle point light particles and γ quanta are emitted during the saddle-to-scission time which is altered due to nuclear dissipation [20]

$$\tau_{ssc} = \tau_{ssc}(\gamma=0)[(1+\gamma^2)^{1/2} + \gamma]. \qquad (4.3)$$

If friction coefficient depends on the excitation energy then the τ_{ssc} interval will effectively depend on the angular mo-

mentum and excitation energy of compound nucleus after the transition of fission barrier. The initial excitation energy at the saddle-to-scission descent stage is assumed to be an average value of excitation energy after presaddle particle and γ-ray emission and excitation energy at the scission point.

The total kinetic energy of fission fragments is a sum of Coulomb interaction energy, kinetic energy at the scission point, and rotational energy

$$E_k = V_{Coul} + A_{rot}^{rel} L(L+1) + E_k^{sc}. \qquad (4.4)$$

Here A_{rot}^{rel} is a rotational constant for relative rotation of two fragments, kinetic energy E_k^{sc} at scission point is of the order of temperature, and relative angular momentum L is determined in the rigid rotation limit. The excitation energy of the compound nucleus at scission point is calculated after subtraction of the energy removed by prescission particles and γ rays from initial total excitation energy. Characteristics of postscission light particles and γ rays are calculated for average excitation energies of fission fragments obtained in the framework of the simplified version of a fission scission point model developed recently [21].

The shape and temperature dependences of friction strength is an important problem in fission dynamics and at present no definite conclusions can be made about its behavior [1,3]. It was found that the energy dependence of dissipation strength reveals threshold character and the dissipation sets up rather rapidly at nuclear excitation energies around ~ 40 MeV [22,2]. In this study we used the following ansatz for the energy dependence of the reduced friction coefficient:

$$\beta(E^*) = \begin{cases} 0 & \text{if } E^* \text{ or } E_{co}^* < E_{th}^* \\ \beta(E_{co}^*)(E^*/E_{co}^*)^p & \text{if } E^* \geq E_{th}^*, \end{cases} \qquad (4.5)$$

where E_{co}^* is an initial excitation energy of compound nucleus, E^* is an excitation energy during evaporation cascade, and the exponent p is considered as an adjusting parameter.

Monte Carlo simulation procedure was used to model in a natural way the timing of the process. For each event the time of transition from equilibrium state over fission barrier is calculated by summing partial life times during sequential cascade decay

$$\tau_{eq \to sd} = \frac{\hbar}{\Gamma_f(t_{N_c})} + \sum_{i=1}^{N_c} \frac{\hbar}{\Gamma_p^i}, \qquad (4.6)$$

where t_{N_c} is average time needed to emit N_c particles before passing barrier and equals the second term of the right side of the equation, N_c is a number of emitted light particles and γ quanta, and Γ_p^i is total particle emission width at the ith cascade step. The presaddle time $T_{eq \to sd}$ is obtained by averaging of $\tau_{eq \to sd}$ over compound nucleus momentum distribution and fission events. The postsaddle fission time $T_{sd \to sc}$ is calculated as an averaged value of τ_{ssc} from Eq. (4.3). The multiplicity distributions and energy spectra of light particles (neutron, proton, α particle, and γ quanta) emitted before passing the saddle point, at the descent stage, and after scission are also calculated.
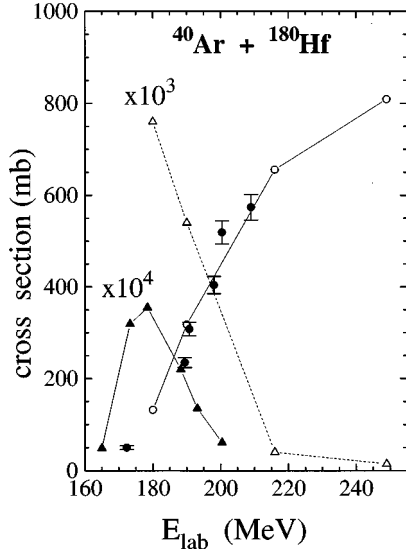
FIG. 3. Comparison between calculated (open symbols) and experimental (solid symbols) values of fission (circles) and evaporation residue cross sections (triangles) for the fusion-fission reaction ^{40}Ar+^{180}Hf. Experimental data are taken from from Ref. [23].
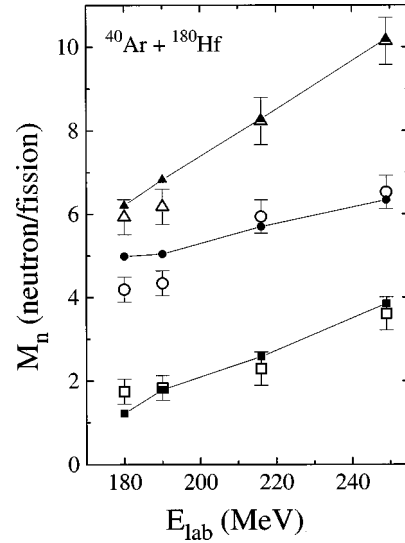

FIG. 4. Experimental (open symbols) and calculated (solid symbols) values of prescission (squares), postscission (circles), and total (triangles) neutron multiplicities.

In Fig. 3 the calculated fission cross section (open circles) is compared with experimental one (solid circles) [23]. The theoretical values of fusion barrier and its position are 142.3 MeV and 11.79 fm, respectively. One can see from Fig. 3 that the model describes well the fission cross section. The calculated ER cross section (open triangles) and the measured σ_{ER} (solid triangles) are also displayed in Fig. 3. In comparison with our previous estimation of the ER cross section [5] the present updated calculation gives significantly lower values. But at the present it is unclear for us how to describe experimental values of σ_{ER} reported in Ref. [23]. Comparison with analysis of σ_{ER} for compound nuclei ^{216}Th and ^{224}Th, presented in Ref. [24], shows that available experimental information about the ER cross section for neutron-deficient Th compound nuclei formed in fusion-fission reactions is insufficient. The values of σ_{ER} provide restrictions on the parameters describing fission width, and we found these parameters to be $\tau_d = 30 \times 10^{-20}$ s, $C_b = 0.95$, $C_a = 1.03$.

Calculated prescission light particle multiplicities are defined as the sum of multiplicities emitted before transition through fission barrier and at descent from the saddle to scission point:

$$M^{\text{pre}} = M^{\text{eq} \rightarrow \text{sd}} + M^{\text{sd} \rightarrow \text{sc}}. \qquad (4.7)$$

With the increase of projectile energy the contribution of particles emitted at the descent stage to total prescission multiplicity increases. Presaddle neutron multiplicities decrease with the increase of compound nucleus spin because the fission barrier decreases as well. There is a strong correlation between the evaporation residue cross section and presaddle neutron multiplicity. Therefore ratio of $M^{\text{eq} \rightarrow \text{sd}}/M^{\text{pre}}$ decreases with increasing fissility of compound nuclei formed in heavy-ion fusion reactions. Comparison of experimental (open symbols) with calculated (solid symbols) values of prescission (squares), postscission (circles), and total (triangles) neutron multiplicities is made in Fig. 4. The model

describes well the experimental dependence of neutron multiplicities on ^{40}Ar energy. From comparison of theoretical and experimental data the parameters describing the energy dependence of the friction coefficient [see formula (4.3)] and the saddle-to-scission time for collective motion without friction [see formula (4.2)] were estimated: β ($E_{\text{co}}^*) = 40 \times 10^{21}$ s^{-1}, $E_{\text{th}}^* = 40$ MeV, $p = 5$, $\tau_{\text{ssc}}(\gamma = 0) = 5 \times 10^{-21}$ s. The averaged slopes of calculated neutron multiplicities as a function of E_{lab} are

$$(dM^{\text{pre}}/dE_{\text{lab}})^{-1} = 27.1 \ \text{MeV/neutron},$$

$$(dM^{\text{post}}/dE_{\text{lab}})^{-1} = 48.8 \ \text{MeV/neutron},$$

$$(dM^{\text{tot}}/dE_{\text{lab}})^{-1} = 17.4 \ \text{MeV/neutron}.$$

The calculated averaged excitation energy at the scission point which originates from the initial excitation energy of the compound nucleus increases almost lineally from 35.6 MeV at $E_{\text{lab}} = 180$ MeV to 59.5 MeV at $E_{\text{lab}} = 249$ MeV.

Theoretical distributions of the presaddle time for four values of ^{40}Ar energies are presented in Fig. 5. With the increase of bombarding energy the width of this distribution decreases and the very long time tail disappears. The averaged fission (prescission) time T_f, evaluated from comparison of experimental data with theoretical calculations, is shown in Fig. 6 (solid squares) together with presaddle time $T_{\text{eq} \rightarrow \text{sd}}$ calculated with friction (solid triangles) and without friction (open triangles). The fission time decreases very slowly with increasing of bombarding energy at $E_{\text{lab}} > 220$ MeV. One can see from Fig. 6 that dissipation hindered fission probability by about two orders of magnitude. There is no other estimation of the fission time scale for the reaction under consideration. We can only compare our result with the fission time scale obtained for the closest compound nucleus ^{221}Pa formed in reaction ^{40}Ar+^{181}Ta at $E_{\text{lab}} = 249$ MeV. In Ref. [4] Hinde et al. obtained a value of T_f of about 5×10^{-20} s, and Siwek-Wilczyńska et al. [25] gave a value of T_f of about 60×10^{-20} s. Our result for com-
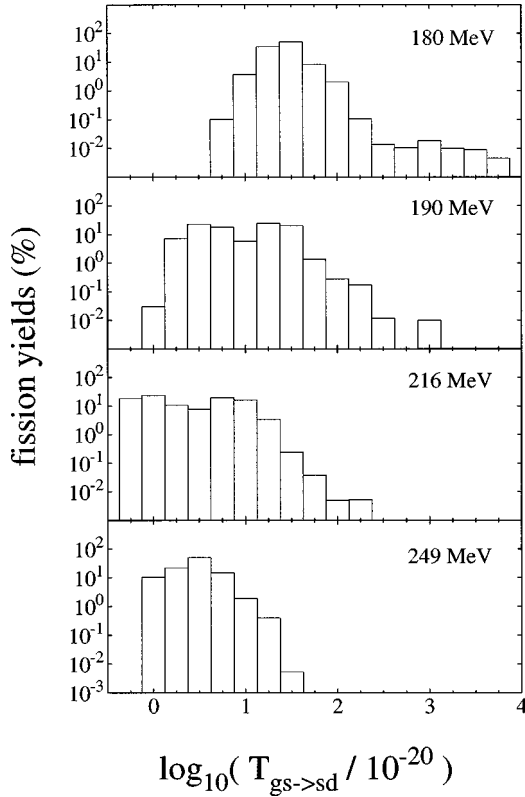
FIG. 5. Calculated distribution of presaddle time for four values of ^{40}Ar energies.

pound nucleus ^{220}Th formed in reaction ^{40}Ar$+^{180}$Hf at the same energy falls between these two estimations ($T_f = 17 \times 10^{-20}$ s).

V. SUMMARY AND CONCLUSION

The results of our measurements of prescission and postscission neutron multiplicities in fusion-fission reaction ^{40}Ar$+^{180}$Hf at $E_{lab} = 249$ MeV are in good agreement with the systematics obtained in Ref. [4]. We think that the local maximum of $M^{pre}(A_{CN})$ at $A_{CN} \sim 220$ (Fig. 13 in Ref. [4]) may be connected with the proximity to the closed neutron shell $N = 126$. The total neutron multiplicity M^{total} obtained in the present work is somewhat higher than that in Ref. [4] and it cannot be completely explained by the difference in excitation energies of the compound nucleus [$E_c^*(^{220}$Th$) - E_c^*(^{221}$Pa$) = 4.1$ MeV].

The measured data were analyzed using the new version of time-dependent statistical model built into the code SCRONMCD [6]. The dynamical effects: retardation of the large scale collective motion, emission of light particles and γ quanta during the saddle-to-scission transition, and deexcitation process of fission fragments are included in the code. From the comparison of the experimental data with model calculations, model parameters were determined and the fission time scale for compound nucleus was extracted. It was found that collective motion along the fission path is over-damped at excitations exceeding the threshold value $E_{th}^* \sim 40$ MeV. This supports the conclusion made in Ref. [22]. The reduced friction coefficient is supposed to depend on excitation energy to describe consistently the prescission
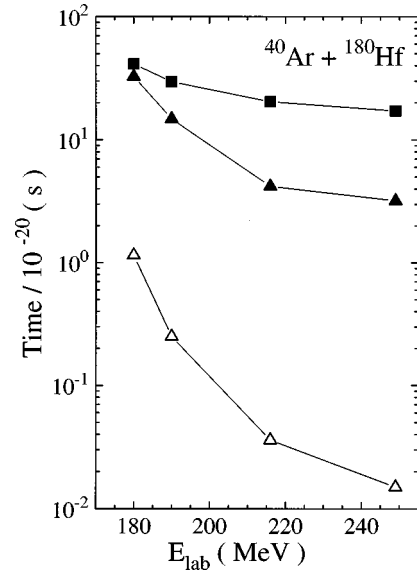

FIG. 6. Averaged prescission time T_f (solid squares) and pre-saddle time $T_{eq\rightarrow sd}$ calculated with friction (solid triangles) and without friction (open triangles) as a funtion of ^{40}Ar-ion energy.

characteristics and evaporation residue cross sections. Calculations were carried out with a large initial value of friction coefficient $\beta(E_{co}^*) = 40 \times 10^{21}$ s^{-1} [$\gamma(E_{co}^*) = 20$] which is constant in the considered projectile energy interval but the effective value of the friction coefficient decreases during the evaporation cascade [see formula (4.5)]. In this case the effective friction coefficient averaged over the prescission neutron cascade decreases with the increase of the initial excitation energy of a compound nucleus in a way similar to the temperature dependence of two-body friction. Although we do not introduce explicitly the dependence of the friction coefficient on nuclear deformation, the effective value of the friction coefficient at the descent stage is greater than that near the equilibrium state due to the energy gain during the descent. Hoffman *et al.* [26] found that their results on the emission of prescission giant dipole resonance γ rays demand that the friction coefficient increases with temperature above the threshold value. However, this temperature-dependent friction ansatz seems to contradict the coordinate-dependent friction ansatz introduced by Fröbrich *et al.* [27]. It was shown recently [28] that both approaches reproduce the main trends of experimental data because only average friction strengths near equilibrium state and at descent are of importance.

The dependence of prescission time on bombarding energy was obtained. In the measured energy interval T_f decreases from 40×10^{-20} s to 17×10^{-20} s. At $E_{lab} > 200$ MeV the descent time from saddle to scission point becomes larger than the presaddle time.

ACKNOWLEDGMENTS

[1] D. Hilscher and H. Rossner, Ann. Phys. (Paris) **17**, 471 (1992).

[2] P. Paul and M. Thoennessen, Annu. Rev. Nucl. Part. Sci. **44**, 65 (1994).

[3] D. Hilscher, I. I. Gontchar, and H. Rossner, Yad. Fiz. **57**, 1255 (1994) [Phys. At. Nucl. **57**, 1187 (1994)].

[4] D. J. Hinde, D. Hilscher, H. Rossner, B. Gebauer, M. Lehman, and M. Wilpert, Phys. Rev. C **45**, 1229 (1992).

[5] A. V. Kuznetsov, V. A. Rubchenya, D. N. Vakhtin, V. G. Lyapin, I. D. Alkhazov, S. V. Khlebnikov, O. I. Osetrov, G. P. Tiourin, W. H. Trzaska, and J. Äystö, Z. Phys. A **354**, 287 (1996).

[6] V. A. Rubchenya, in *Proceedings of the International Conference on Large-Scale Collective Motion of Atomic Nuclei*, Brolo, Messina, Italy, 1996, edited by G. Giardina, G. Fazio, and M. Lattuada (World Scientific, Singapore, 1997), p. 534.

[7] W. H. Trzaska *et al.*, in *Proceedings of the International Conference LEND95*, St. Petersburg, 1995, edited by Yu. Oganessian, W. von Oertzen, and R. Kalpakchieva (World Scientific, Singapore, 1995), p. 246.

[8] H.-G. Ortlepp *et al.*, in *Proceedings of the International School-Seminar on Heavy Ion Physics*, Dubna, 1993, edited by Yu. T. S. Oganessian *et al.* (JINR, Dubna, 1993), Vol. 2, p. 466.

[9] A. V. Kuznetsov, I. D. Alkhazov, D. N. Vakhtin, V. G. Lyapin, V. A. Rubchenya, W. H. Trzaska, K. Loberg, and A. V. Daniel, Nucl. Instrum. Methods Phys. Res. A **346**, 259 (1994).

[10] V. E. Viola, K. Kwiatkowski, and M. Walker, Phys. Rev. C **31**, 1550 (1985).

[11] A. V. Daniel and V. Yu. Perov, in *Proceedings of a Specialist meeting "Intemediate Energy Nuclear Data: Models and Codes,"* Issy-Les-Moulineaux, France, 1994, OECD 1994 (unpublished), pp. 301–312.

[12] A. V. Daniel, E. M. Kozulin, and A. V. Kuznetsov, JINR Report No. P3-92-325, Dubna, 1992.

[13] W. J. Swiatecki, Nucl. Phys. **A376**, 275 (1982).

[14] Yi-Sin Shi and W. J. Swiatecki, Phys. Rev. Lett. **54**, 300 (1985).

[15] V. V. Pashkevich, Nucl. Phys. **A169**, 275 (1971).

[16] X. Campi and S. Stringari, Z. Phys. A **309**, 239 (1983).

[17] H. A. Kramers, Physica (Amsterdam) **7**, 284 (1940).

[18] P. Grangé, S. Hassani, H. A. Weidenmüller, A. Gavron, J. R. Nix, and A. J. Sierk, Phys. Rev. C **34**, 209 (1986).

[19] A. V. Ignatyuk, G. N. Smirenkin, and A. S. Tishin, Yad. Fiz. **21**, 485 (1975) [Sov. J. Nucl. Phys. **21**, 255 (1975)].

[20] H. Hofmann and J. R. Nix, Phys. Lett. **122B**, 117 (1983).

[21] P. P. Jauho, A. Jokinen, M. Leino, J. M. Parmonen, H. Penttilä, J. Äystö, K. Eskola, and V. A. Rubchenya, Phys. Rev. C **49**, 2036 (1994).

[22] M. Thoennessen and G. F. Bertsch, Phys. Rev. Lett. **71**, 4303 (1993).

[23] H.-G. Clerc, J. G. Keller, C.-C. Sahm, K.-H. Schmidt, H. Schulte, and D. Vermeulen, Nucl. Phys. **A419**, 571 (1984).

[24] P. Fröbrich and I. I. Gontchar, Phys. Rep. **292**, 131 (1998).

[25] K. Siwek-Wilczyńska, J. Wilczyński, R. H. Siemssen, and H. W. Wilschut, Phys. Rev. C **51**, 2054 (1995).

[26] D. J Hofman, B. B. Back, and P. Paul, Phys. Rev. C **51**, 2597 (1995).

[27] P. Fröbrich, I. I. Gontchar, and N. D. Mavlitov, Nucl. Phys. **A556**, 281 (1993).

[28] I. Gontchar and L. A. Litnevsky, Z. Phys. A **359**, 149 (1997).